Radiative Cooling Potential Maps for Spain

Roger Vilà, Lídia Rincón, Marc Medrano, Albert Castell

Sustainable Energy, Machinery and Buildings (SEMB) Research Group, INSPIRES Research Centre, Universitat de Lleida, Pere de Cabrera s/n, 25001 Lleida (Spain)

Abstract

Radiative cooling is a novel technology which provides cooling power by emitting thermal radiation using the sky as a heat sink. Under proper conditions, net radiative cooling power of an ideal surface can be expressed as the difference between the emitted longwave radiation of a black surface minus the infrared radiation emitted by the atmosphere and absorbed by the surface. This atmospheric radiation depends on the local conditions. A continuous map of the radiative cooling potential in Spain has been prepared using two interpolation methods: Inversed Distance Weighted (IDW) and Kriging. The results obtained showed an average cooling potential of 55-60 W/m^2. Climate change, under different IPCC scenarios, do not have a big impact in the average capacity to do radiative cooling in Spain.

Keywords: radiative cooling, cooling potential, renewable energy, spatial interpolation, climate change

1. Introduction

The contribution of the greenhouse gases to climate change, as a result of the human activity, has reached a consensus among the scientific community. Global environmental awareness is currently increasing among society; this concern is reflected in public policies such as the Project Europe 2030 (*Project Europe 2030*, 2010). In the European Union, consumption in buildings accounts for 40% of the total energy demand and 36% of CO_2 emissions (European Comission, n.d.). In residential buildings this energy is mostly used for space conditioning purposes and domestic hot water (DHW). In this context, the share of renewable energies only accounts for 17.5%.

Radiative cooling is a novel, renewable and clean technology for space cooling. Radiative cooling is the process by which a surface -named radiative cooler- cools down by emitting thermal radiation towards the outer space taking advantage of the infrared atmospheric window transparency in the 7-14 μm range (Vall and Castell, 2017).

Under nighttime conditions, in the absence of solar radiation, radiative cooling power of a radiative cooler, at temperature T_s, can be expressed as eq. 1. The first term of the equation refers to the infrared energy radiated by the surface, the second term corresponds to the infrared radiation emitted by the atmosphere and absorbed by the surface, q_{cond} and q_{conv} are non-radiative heat exchanges. The emittance (ε_s) of ideal surfaces is equal to one, maximizing radiative cooling, if the surface is assumed to work at ambient temperature it can be expressed as eq. 2. If a radiative cooler is designed to work at ambient temperature, convective and conductive heat exchanges are minimized and radiative power is expressed as eq. 3 (Chang and Zhang, 2019).

$$q_c(T_s) = \varepsilon_s \sigma T_s^4 - \varepsilon_s \varepsilon_{sky} \sigma T_a^4 - q_{cond} - q_{conv} \quad [W/m^2] \quad \text{(eq. 1)}$$

$$q_{c,ideal}(T_a) = \sigma T_a^4 (1 - \varepsilon_{sky}) - q_{cond} - q_{conv} \quad [W/m^2] \quad \text{(eq. 2)}$$

$$q_{c,ideal}(T_a) = \sigma T_a^4 (1 - \varepsilon_{sky}) \quad [W/m^2] \quad \text{(eq. 3)}$$

Infrared radiation from the atmosphere depends on the local conditions. As a consequence, radiative cooling potential varies between zones. Up until this time, it doesn't exist, in European countries, a source of field values of radiative cooling potential based on the location. Prediction of radiative cooling potential in different areas could become an aid to drive public policies on the usage of renewable energies.

Based on statistical models, and using available meteorological data for small group of points, the prediction of radiative cooling potential can be obtained for a whole region or country. Chang and Zhang (Chang and Zhang, 2019) modeled incoming infrared radiation in China and studied the radiative cooling potential using Kriging interpolation. Li et al. (Li et al., 2019) used Inverse Distance Weighting (IDW) interpolation to generate radiative cooling potential maps in USA. In this study we used both geostatistical methodologies to predict radiative cooling maps in Spain in order to discover what is the maximum potential of radiative cooling in Spain and which are the regions that have more potential. This study is complemented with the exploration of the evolution of radiative

doi:10.18086/eurosun.2020.09.01 Available at http://proceedings.ises.org

cooling potential in Spain under the context of climate change.

2. Methods

2.1. Data Acquisition

Climate data was obtained from the Meteonorm database. Meteonorm is a software used in energy simulation of buildings and solar applications that combines global meteorological data, space interpolations and stochastic weather generation (Remund et al., 2019).

The data obtained corresponded to the period 1991-2010 and each point in the sample contained hourly weather data for each day in a year. These data included ambient temperature, T_a and long-wave radiation from the atmosphere, q_{atm}, used in the calculation of radiative cooling. The sample was made up of data from 63 points in Spain. The number of points, 63, was determined by the total of points available in Metonorm, of which 52 belonged to the peninsular region, 3 to the Balearic Islands and 8 to the Canary Islands.

The evolution of the nocturnal potential of radiative cooling in the context of climate change was also studied using Meteonorm's data based on the emission scenarios presented in the fourth IPCC assessment report. The fifth assessment report presented new scenarios, the SRC scenarios; however, the fourth IPCC scenarios were chosen as for the SRC scenarios data was only available for big urban areas, which would have meant a very small dataset. For the Fourth Assessment Report (AR-4) based scenarios, data was available in all of the 63 points. Data was obtained from the three different scenarios available in Meteonorm: B1 (low emissions), A1B (middle emission) and A2 (high emission) (Solomon et al., 2007). Data from 2020 to 2050 maintained the same structure described above.

2.2. Data Preparation

Data preprocessing and data cleaning, as well as the statistical analysis and spatial predictions, were done with Rstudio version 1.3.

In order to obtain the nighttime radiative cooling (RC) potential, once the cleaning was performed, night values of the dataset were filtered. The maximum RC potential for each hour was calculated using the eq. 4. At each point of the sample the mean was calculated to know the annual average value of the radiative cooling potential.

$$q_{c,ideal}(T_a) = \sigma T_a^4 - q_{atm}\ [W/m^2\ ] \quad \text{(eq. 4)}$$

Some authors affirm that one requirement for Kriging is a normal distribution of the data (Hengl, n.d.), being necessary a transformation of the data in case it is not followed. Other authors say that there is no guarantee that doing this pre-transformation will result in better biased estimators (Villatoro et al., 2008). It was verified, using a Chi-Squared and a Shapiro-Wilk tests, that the data followed a normal distribution.

2.3. Interpolation models and validations

Two interpolation models have been used to predict the potential in Spain: Inverse Distance Weighting (IDW) and Kriging.

IDW is a deterministic model which assumes that close points are more correlated than others, and the influence of sample points to an unknown point decreases with a power of the distance. IDW estimator is computed as (Li et al., 2019):

$$\hat{z}(s_0) = \frac{\sum_i^N w(s_i) \cdot z(s_i)}{\sum_i^N w(s_i)} \quad \text{(eq. 5)}$$

Where $\hat{z}(s_0)$ is the predicted value at a point s_0, $z(s_i)$ is the sample value at station s_i, N is the number of sample points and $w(s_i)$ is the weight of station $s_i$which is defined as the Euclidean distance to a p power.

$$w(s_i) = \|s_i - s_0\|^{-p} \quad \text{(eq. 6)}$$

Kriging is a stochastic model based on the covariance of the sample point (Scheuerer et al., 2013) where predictions at an unknown point are a weighted linear combination of values at known points. Same as the IDW, it assumes that the points closer to the point of study have the greatest influence on the prediction, having a greater

autocorrelation; while with distant points it becomes independent. The main difference is that in Kriging weights are not only based on this distance but they are also chosen to ensure an unbiased model and a minimum variance, adding complexity to the model. The quantification of these weights is achieved through the use of variograms. In the case study, theoretical variograms were adjusted to the data so that the error was minimal. The variogram is defined as the variance of the difference between field values at two locations (Hengl, n.d.):

$$\gamma(h) = \frac{1}{2} E[(z(s_i) - z(s_i + h))^2]$$

Where $\gamma(h)$ is the theoretical variogram, $z(s_i)$ is the value of the target variable and $z(s_i + h)$ is the value of neighboring points at distance h.

Predictions were made in both models at a total of 296.197 new points. In order to assess the fit of the models, Leave-one-out cross-validation (LOOCV) was applied. LOOCV makes predictions at points in the sample using all data except that of the point in question; the process is repeated for all points in the sample. The differences between the predicted values and the observed values were then compared and the coefficients of determination (R^2) and root-mean-square deviation (RMSD) were computed.

3. Results and discussion

3.1. IDW and Kriging. Interpolation: 1991-2010 period.

Fig. 1 shows the spatial prediction maps of annual nocturnal radiative cooling potential for Spain. In both models, spatial distribution can be divided into a central area and the Canary Islands with the highest potential, the Mediterranean coast - south and east - with medium potential and the North Atlantic and Cantabrian area with the lowest potential in conjunction with the Balearic Islands.

Both models predict similar average annual values. The results of the Kriging model are slightly higher: the average night-time potential across the country is 59.89 W/m^2 while the IDW model predicts an average of 58.89 W/m^2. The maximum and minimum values of the Kriging interpolator are 70.88 W/m^2 and 45.6 W/m^2, respectively, while for the IDW model, these values are 70.82 W/m^2 and 45.4 W/m^2.

Cross-validation analyzed the goodness of each of the models. R^2 of the Kriging model is 0.71 and the RMSE is 3.05 W/m^2. In the case of IDW, it has a slightly worse performance: the value of R^2 is 0.61 and the RMSD is equal to 3.64 W/m^2.

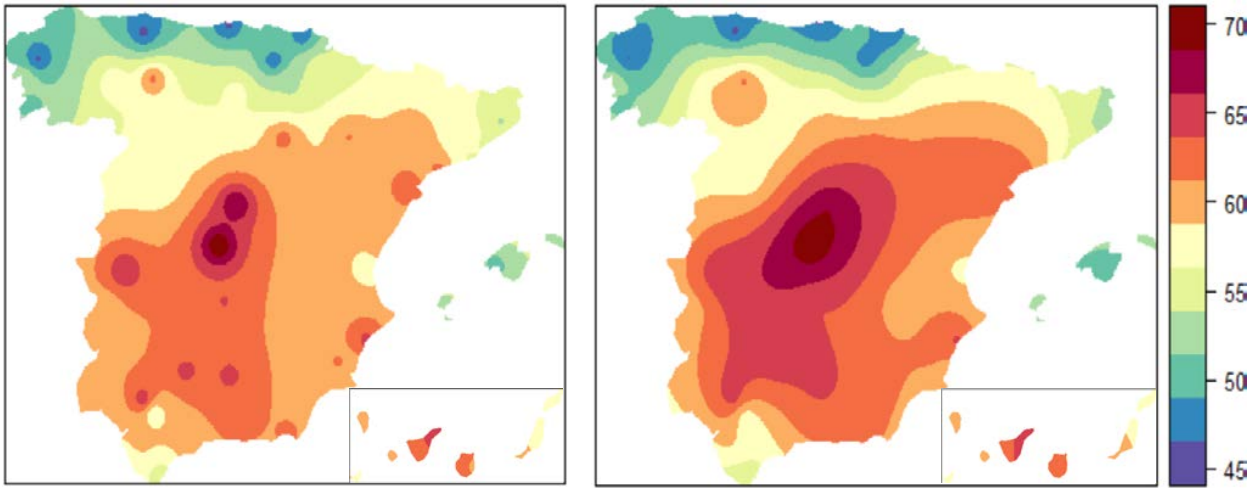

Fig. 1. Map of distribution of anual average nighttime radiative cooling potential [W/m^2] . Two models have been used IDW (left) and Kriging (right).

It is also noteworthy the phenomenon known as "bull's eyes" that appears on the map of the IDW model, represented by unrealistic circular patterns around the area of influence of the sampling points. The Kriging map, on the other hand, presents smoother transitions that pick up the variability of the different points.

3.2. IPCC scenarios. Prediction of radiative cooling evolution.

IPCC scenarios have been interpolated using the Kriging model. They predict a drop of radiative cooling potential with respect to 1991-2010 results. Maps show that the potential of the regions to produce radiative cooling does not vary between 2020 and 2050 (Fig. 2, Fig. 3, Fig. 4), remaining almost constant. For example, the average potential in 2020 within the A1B scenario is 55.67 W/m^2 while in 2050 it is 55.64 W/m^2. In this scenario the maximum and minimum values were 61.43 W/m^2 and 49.46 W/m^2 in 2020 and, 61.60 W/m^2 and 44.46 W/m^2 in 2050. Table 1 lists these summary metrics for the different scenarios. It can be seen that the results converge in the three scenarios, with no significant differences among them. Two main regions can be distinguished: one with higher potential formed by the central regions, the south-west, north-east and the Canary Islands; and the other region, with lower potential, formed by the north, the east and south-east coast and the Balearic Islands.

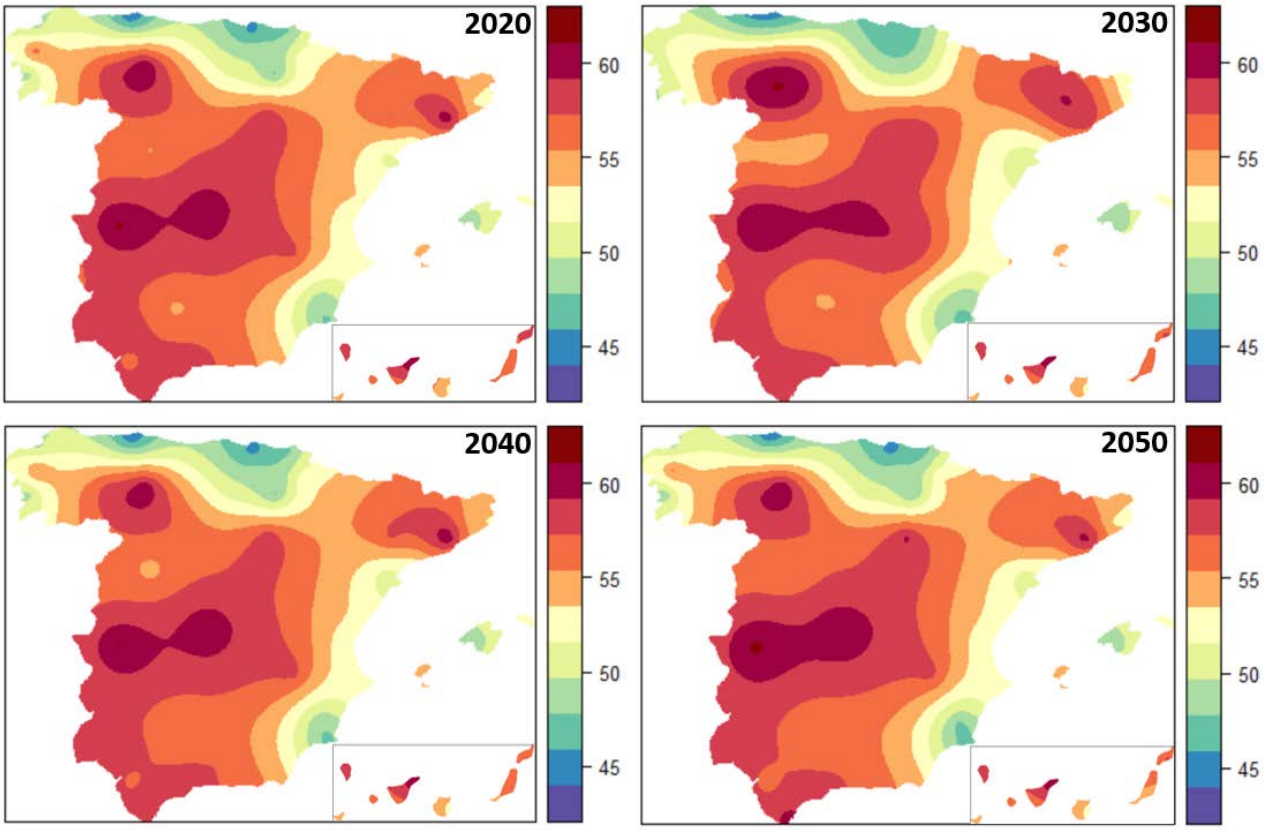

Fig. 2. Map of predictions of nighttime radiative cooling potential [W/m^2] for the period 2020-2050 based on the scenario A1B from the IPCC.

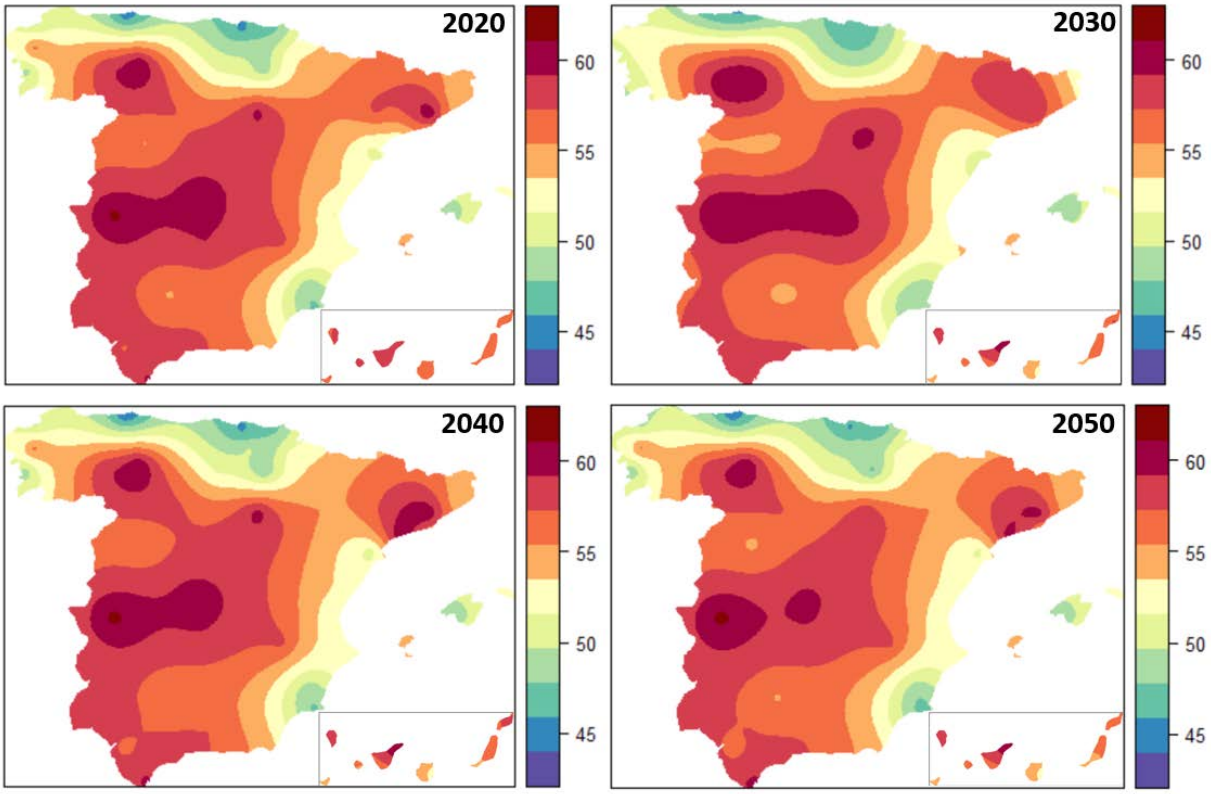

Fig. 3. Map of predictions of nighttime radiative cooling potential [W/m^2] for the period 2020-2050 based on the scenario A2 from the IPCC.

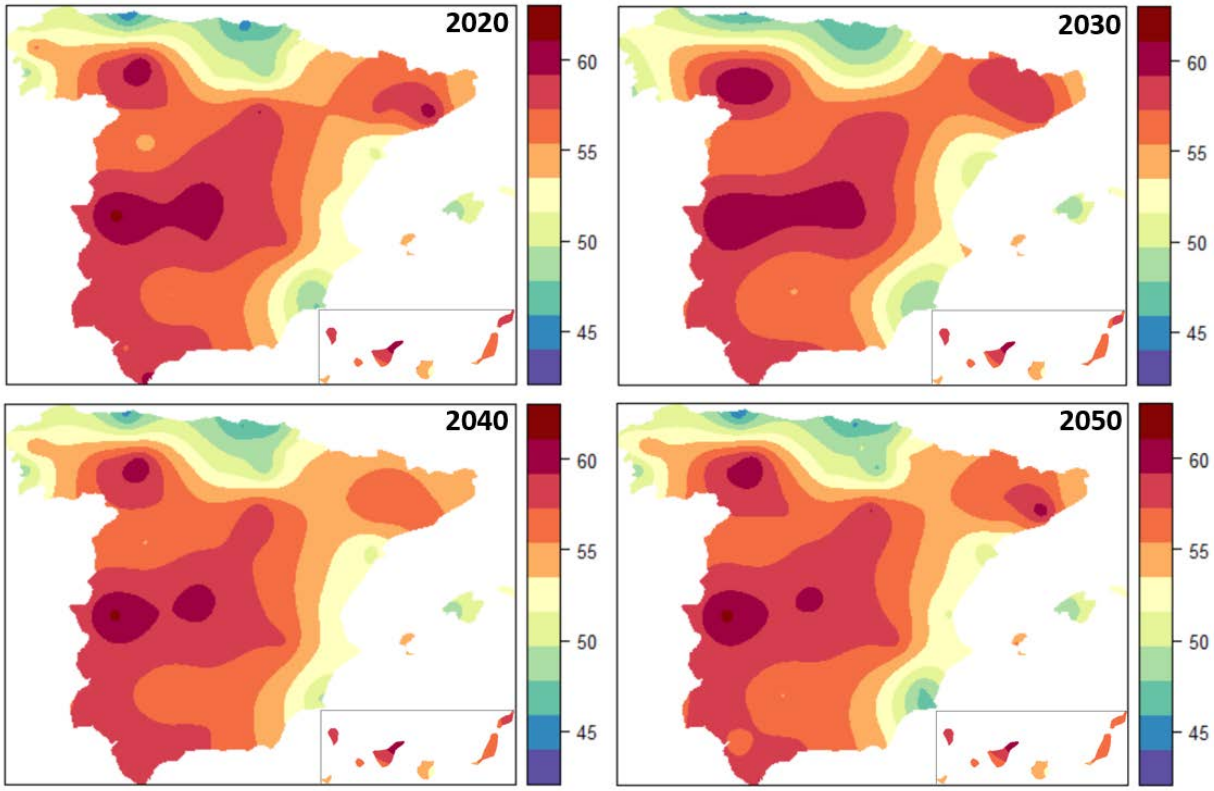

Fig. 4. Map of predictions of nighttime radiative cooling potential [W/m^2] for the period 2020-2050 based on the scenario B1 from the IPCC.

Tab. 1. *Summary metrics of the prediction models*

Year	Scenario	Min	Max	Average	R^2	RMSD
2020	A1B	44.46	61.43	55.67	0.60	2.83
2030		44.76	61.16	55.53	0.61	2.84
2040		44.36	61.21	55.61	0.63	2.75
2050		44.49	61.60	55.64	0.62	2.81
2020	A2	44.74	61.62	55.90	0.63	2.77
2030		45.45	60.69	55.59	0.60	2.84
2040		44.29	61.75	55.83	0.59	2.96
2050		44.55	61.77	55.64	0.60	2.89
2020	B1	44.30	61.73	55.78	0.61	2.85
2030		45.56	60.95	55.77	0.60	2.90
2040		45.17	61.68	55.69	0.47	3.28
2050		44.43	61.71	55.50	0.60	2.88

From the sample values, in both A1B and A2 scenarios, temperature increases over 1°C while this increase is less than 0.5°C in the B1 scenario. As a result of this increase in temperature (Fig. 5), the infrared radiation emitted by the radiative cooler slightly increases. The infrared radiation from the atmosphere –and absorbed by the radiative cooler– also increases (Fig. 6), compensating this radiation emitted by the radiative cooler due to the surface temperature. As a result of this balance, the average radiative cooling remains constant throughout the studied years (Fig. 7).

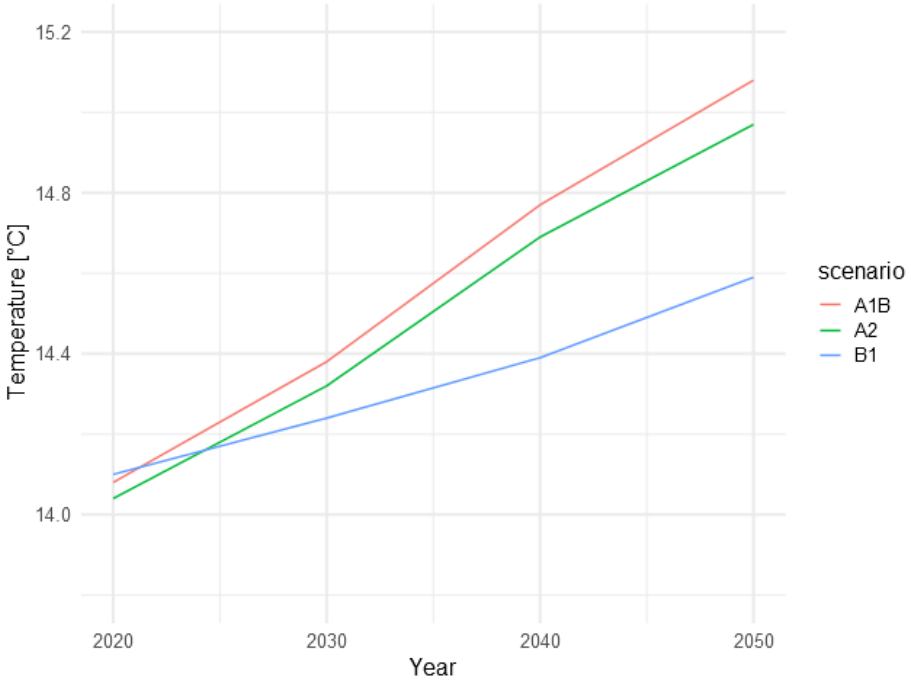

Fig. 5. Evolution of the mean surface temperature for different IPCC scenarios.

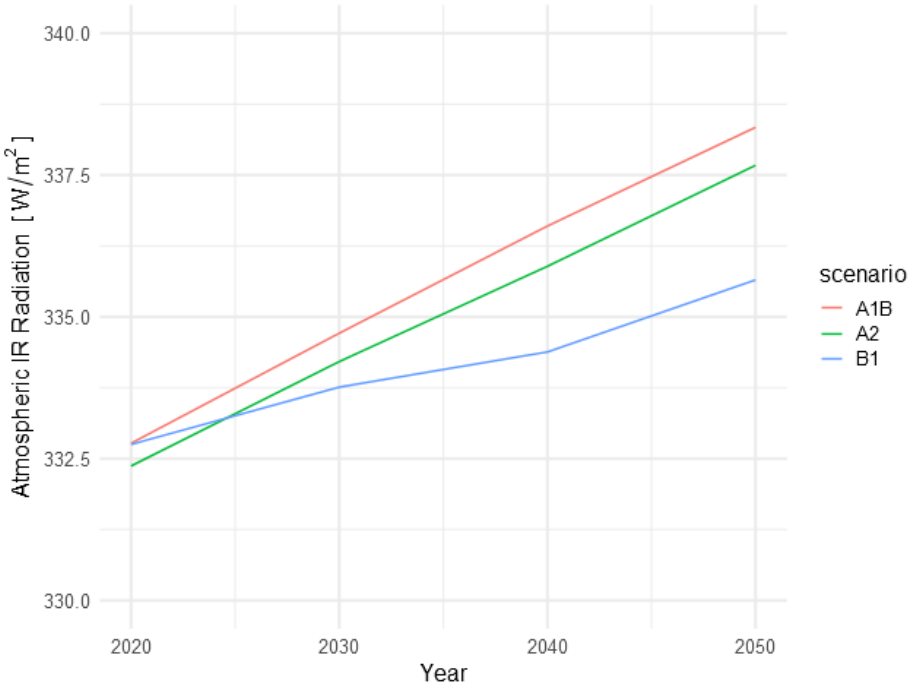

Fig. 6. Evolution of the infrared radiation coming from atmosphere and absorbed by the emitting surface for different IPCC scenarios.

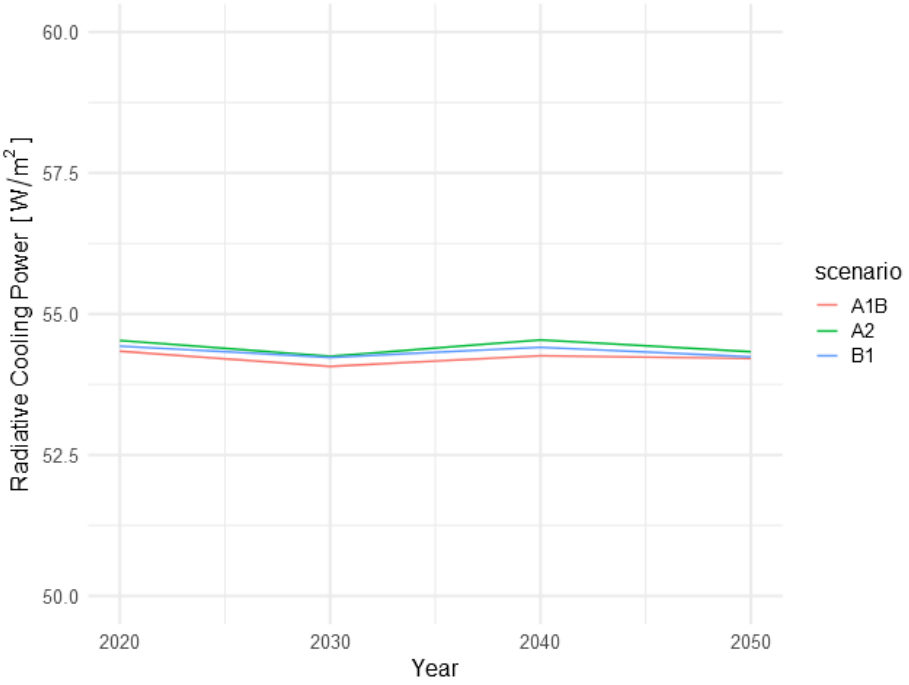

Fig. 7. The evolution of the net radiative cooling power, computed as the difference between the emitted radiation and the absorbed radiation from the atmosphere, remains constant under different IPCC scenarios.

4. Conclusions

This work has presented the nocturnal potential in Spain of a renewable technology for cold production: radiative cooling. To determine this potential two interpolation models have been used: IDW and Kriging. The results show that the average annual capacity for surfaces that behave like an ideal black body is around 58-60 W/m^2; the actual case will remain below these estimations. Radiative cooling potential depends on the location The most favorable areas for radiative cooling are the central regions and the Canary Islands, while the north and the Balearic Islands have lower predictions. Of the two models used, the Kriging model appears to be a better model than the IDW. In IDW, source points have a strong influence on the final predictions showing, in the maps, unrealistic patterns around them; in Kriging, predictions present smoother transition.

Predictions of the evolution of the potential have also been made based on different emission scenarios from the fourth IPCC report. Under these scenarios, the average annual night potential is slightly reduced to 55-56 W/m^2. These scenarios predict a temperature rise of 0.49°C, in the most favorable scenario, and 1°C in the most unfavorable between 2020 and 2050. An increase in ambient temperature does not mean an increase in potential as it is balanced out by an increase in long-wave atmospheric radiation.

All three scenarios have converged to similar radiative cooling nocturnal values. Despite the slight reduction in potential, climate change does not have a significant impact on the average capacity for radiative cooling in Spain. In these scenarios the northern region of the country is distinguished from the rest of the country.

5. Acknowledgments

The work was partially funded by the Spanish government under grant agreement RTI2018-097669-AI00 (Ministerio de Ciencia, Innovación y Universidades). The authors would like to thank Generalitat de Catalunya for the project grant given to their research group (2017 SGR 659).

6. References

Chang, K., Zhang, Q., 2019. Modeling of downward longwave radiation and radiative cooling potential in China. Journal of Renewable and Sustainable Energy 11, 066501. https://doi.org/10.1063/1.5117319

European Comission, n.d. Energy performance of buildings directive. URL https://ec.europa.eu/energy/en/topics/energy-efficiency/energy-performance-of-buildings/energy-performance-buildings-directive#documents (accessed 1.23.18).

Hengl, T., n.d. A Practical Guide to Geostatistical Mapping 165.

Li, M., Peterson, H.B., Coimbra, C.F.M., 2019. Radiative cooling resource maps for the contiguous United States. Journal of Renewable and Sustainable Energy 11, 036501. https://doi.org/10.1063/1.5094510

Project Europe 2030: challenges and opportunities : a report to the European Council by the Reflection Group on the Future of the EU 2030, 2010. . Publications Office of the European Union, Luxemburg.

Remund, J., Müller, S., Kunz, S., Huguenin-Landl, B., Studer, C., Cattin, R., 2019. Meteonorm. Meteotest, Switzerland.

Scheuerer, M., Schaback, R., Schlather, M., 2013. Interpolation of spatial data – A stochastic or a deterministic problem? Eur. J. Appl. Math 24, 601–629. https://doi.org/10.1017/S0956792513000016

Solomon, S., Intergovernmental Panel on Climate Change, Intergovernmental Panel on Climate Change (Eds.), 2007. Climate change 2007: the physical science basis: contribution of Working Group I to the Fourth Assessment Report of the Intergovernmental Panel on Climate Change. Cambridge University Press, Cambridge ; New York.

Vall, S., Castell, A., 2017. Radiative cooling as low-grade energy source: A literature review. Renewable and Sustainable Energy Reviews 77, 803–820. https://doi.org/10.1016/j.rser.2017.04.010

Villatoro, M., Henríquez, C., Sancho, F., 2008. Comparación de los interpoladores IDW y Kriging en la variación espacial de pH, Ca, CICE y P del suelo. Agronomía Costarricense 12.